

EUROPEAN ORGANIZATION FOR NUCLEAR RESEARCH
CERN-SL DIVISION

CERN-SL-2002- 039 (AP)

Direct Measurement of Resonance Driving Terms at SPS at 26 GeV

M. Hayes, F. Schmidt and R. Tomas

In 2001 a series of experiments has been performed at the SPS at an energy of 26 GeV to measure resonance driving terms. Theory predicts that these terms can be determined by harmonic analysis of BPM data recorded after applying single kicks. This analysis works equally well for linear and non-linear diagnostics of accelerators. Results of the experiments are presented, including a direct measurement of resonance driving terms and a comparison to the theory.

*8th European Particle Accelerator Conference, 3-7 June 2002
Paris, France*

Geneva, Switzerland
25 June, 2002

Direct Measurement of Resonance Driving Terms at SPS at 26 GeV

M. Hayes, F. Schmidt and R. Tomás, CERN, Geneva, Switzerland.

Abstract

In 2001 a series of experiments has been performed at the SPS at an energy of 26 GeV to measure resonance driving terms. Theory predicts that these terms can be determined by harmonic analysis of BPM data recorded after applying single kicks. This analysis works equally well for linear and non-linear diagnostics of accelerators. Results of the experiments are presented, including a direct measurement of resonance driving terms and a comparison to the theory.

1 INTRODUCTION

Since many years perturbation theory [1] and more recently the Normal Form [2, 3] techniques have been used to understand nonlinear motion of single particles in hadron accelerators. This has proven to be very useful in the design phase of an accelerator. When it comes to existing machines these sophisticated tools have been rarely in use up to now. In part this is due to the complexity of the theory but also due to the fact that a nonlinear model of the accelerator cannot be easily anticipated. Checking such a model experimentally [4] may prove even more difficult.

One well documented attempt to overcome this problem has been made by Bengtsson [5]. In the framework of the first order perturbation theory he has studied how the real spectra from tracking or experimental turn-by-turn data can be related to resonances. This study has stopped short of a complete solution. An important prerequisite to his analysis was a tune measurement technique superior to the standard FFT [6]. Similar attempts were performed in the field of celestial mechanics [7].

Recently, new techniques were developed [8], allowing an even more precise determination of the tunes. It seems therefore appropriate to review the link between experimental data and theoretical models. The frequency map analysis by Laskar [8] can be used not only to derive the tune, but also to find spectral lines in descending order of magnitude. It has already been shown how these spectra can be applied to remove from a sequence of tracking data unwanted regular complexity. Moreover, this method has been successfully used, again in tracking simulations, to correct resonances excited by sextupoles [9].

In this article we summarise our SPS experiments in 2001 which were done in the quest to establish this method as a tool for routine use in the control room.

2 THEORY

The turn-by-turn single particle motion in normalised coordinates to first order in the non-linearities is given by [10]

$$\hat{x}(N) - i\hat{p}_x(N) = \sqrt{2I_x} e^{i(2\pi\nu_x N + \psi_{x_0})}$$

$$-2i \sum_{jklm} j f_{jklm} (2I_x)^{\frac{j+k-1}{2}} (2I_y)^{\frac{l+m}{2}} \times e^{i[(1-j+k)(2\pi\nu_x N + \psi_{x_0}) + (m-l)(2\pi\nu_y N + \psi_{y_0})]} \quad (1)$$

where I_x and I_y are the horizontal and vertical actions, ψ_{x_0} and ψ_{y_0} are the horizontal and vertical initial phases, ν_x and ν_y are the horizontal and vertical tunes including the amplitude dependent detuning and the factors f_{jklm} are the generating function terms. These are related to the Hamiltonian terms h_{jklm} by the following expression,

$$f_{jklm} = \frac{h_{jklm}}{1 - e^{-i2\pi[(j-k)\nu_x + (l-m)\nu_y]}} \quad (2)$$

Note that the term f_{jklm} drives the resonance ($j-k, l-m$). The Hamiltonian terms are defined by the following expansion of the non-linear Hamiltonian,

$$H = \sum_{jklm} h_{jklm} (2I_x)^{\frac{j+k}{2}} (2I_y)^{\frac{l+m}{2}} \times e^{-i[(j-k)(\psi_x + \psi_{x_0}) + (l-m)(\psi_y + \psi_{y_0})]} \quad (3)$$

where ψ_x and ψ_y are the horizontal and vertical angle variables. Eqs. 1 and 2 suggest that a FFT of the turn-by-turn complex signal can be used to measure the generating function and the Hamiltonian terms. The spectral line ($1-j+k, m-l$) depends only on the term f_{jklm} . By line (m, n) we mean the spectral line with frequency $m\nu_x + n\nu_y$. In a real machine the complex signal is constructed from two pick-ups with 90° phase advance.

The Hamiltonian and the generating function terms depend on the longitudinal location where they are calculated. To understand how they vary along the ring the values of a Hamiltonian term at both sides of a source of non-linearity are compared. Prior to this element the term is h_{jklm}^1 and after it is h_{jklm}^2 . The non-linearity contributes to the first case with the quantity k_{jklm} and to the second case with the quantity $e^{-i2\pi[(j-k)\nu_x + (l-m)\nu_y]} k_{jklm}$ because the element has moved to the end of the lattice. Therefore the relation between the two Hamiltonian terms is expressed as

$$h_{jklm}^2 = h_{jklm}^1 + (e^{-i2\pi[(j-k)\nu_x + (l-m)\nu_y]} - 1) k_{jklm} \quad (4)$$

the equivalent relation between the generating function terms is given by

$$f_{jklm}^2 = f_{jklm}^1 - k_{jklm} \quad (5)$$

These relations state that the amplitude of these terms changes abruptly at the location of the sources. Their amplitudes remain constant along sections free of sources. This feature is very important since it allows the localisation of multipolar kicks.

In a real machine the beam is not a single particle but a particle distribution and processes like the beam decoherence change the Fourier spectrum of the turn-by-turn motion. The effect of the decoherence due to amplitude detuning has been described in [11]. The relevant conclusion is that the spectral line (m,0) of a decohered signal is reduced by a factor of $|m|$ compared to the single particle case.

3 MEASUREMENT OF COUPLING

The technique of coupling correction involves measuring the amplitudes of the coupling lines, normalised to the amplitude of the fundamental line, as a function of the strength of the skew quadrupoles. The optimum setting of the skew quadrupoles is then inferred by finding the minimum coupling line amplitude. Previously a different slope at either side of the minimum was found [11]. The theory is now revised to explain this puzzle and a better observable has been found. The turn-by-turn horizontal and vertical coordinates in first order in the coupling resonance term f_{1001} are given by

$$\begin{aligned} \hat{x}(N) - i\hat{p}_x(N) &= \sqrt{2I_x}e^{i(2\pi\nu_x N + \psi_{x0})} \\ &\quad - 2if_{1001}\sqrt{2I_y}e^{i(2\pi\nu_y N + \psi_{y0})}, \\ \hat{y}(N) - i\hat{p}_y(N) &= \sqrt{2I_y}e^{i(2\pi\nu_y N + \psi_{y0})} \\ &\quad - 2if_{1001}^*\sqrt{2I_x}e^{i(2\pi\nu_x N + \psi_{x0})}. \end{aligned} \quad (6)$$

From these equations it can be seen that the normalised amplitude of the vertical tune line from the horizontal plane is $2\sqrt{I_y/I_x}|f_{1001}|$ and the normalised amplitude of the horizontal tune line from the vertical plane is $2\sqrt{I_x/I_y}|f_{1001}|$. Therefore the best way to measure $|f_{1001}|$ independently of the actions is multiplying the former two observables. Thus,

$$2|f_{1010}| = \sqrt{\frac{\text{line}(0,1)_H \text{line}(1,0)_V}{\text{line}(1,0)_H \text{line}(0,1)_V}}. \quad (7)$$

In fig. 1 this new observable is plotted versus the strength of the skew quadrupoles together with the prediction from the model and two linear fits. The fitted slopes are indicated in the figure as well. The agreement between measurement and prediction is excellent and the slopes of the tangents are the same on both sides of the minimum.

4 MEASUREMENT OF SEXTUPOLAR RESONANCE TERMS

To measure sextupolar resonance driving terms the beam is kicked to different amplitudes and the turn-by-turn complex signal is Fourier analysed to obtain the amplitudes of the different spectral lines. For every pick-up the normalised amplitudes of the sextupolar spectral lines are plotted versus kick strength and a line is fitted constrained to go through the origin. As an illustration a plot from this procedure is shown in fig. 2 for a particular pick-up and for

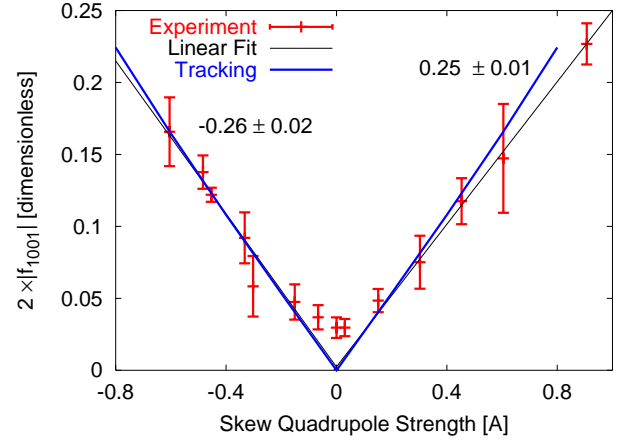


Figure 1: Coupling resonance term versus skew quadrupole strength. Results from experiment and tracking.

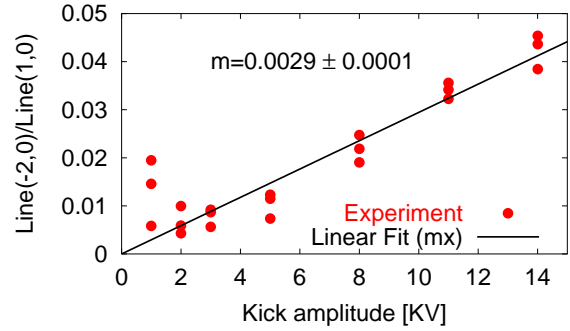


Figure 2: Normalised amplitude of the spectral line (-2,0) versus horizontal kick amplitude for one pick-up.

the spectral line (-2,0). Three measurements for every kick strength were done to assess random errors. The slope of the fitted line is related to the corresponding resonance term in the following way,

$$\begin{aligned} |f_{3000}| &= \frac{1}{6} \frac{m_{(-2,0)}}{0.094} [\text{mm}^{-1/2}], \\ |f_{1200}| &= \frac{1}{2} \frac{m_{(2,0)}}{0.094} [\text{mm}^{-1/2}]. \end{aligned} \quad (8)$$

where the m is the measured slope and its subscript denotes the spectral line from which this slope originates. The factor 0.094 is the calibration of the horizontal kicker in units of $\text{mm}^{1/2}/\text{KV}$. These relations hold as far as the beam does not experience any decoherence. When the centroid oscillations are completely damped due to decoherence caused by amplitude detuning the spectral lines ($\pm 2,0$) are reduced by a decoherence factor of 2 [11]. The sextupolar resonance terms are measured for different machine set-ups. The first set-up was the baseline machine with the nominal tunes $Q_x = 26.62$ and $Q_y = 26.58$. The amplitude detuning was compensated with octupoles to avoid additional decoherence of the signal. In fig. 3 the measured amplitude of the sextupolar resonance terms f_{3000} is plotted versus the longitudinal position together with the

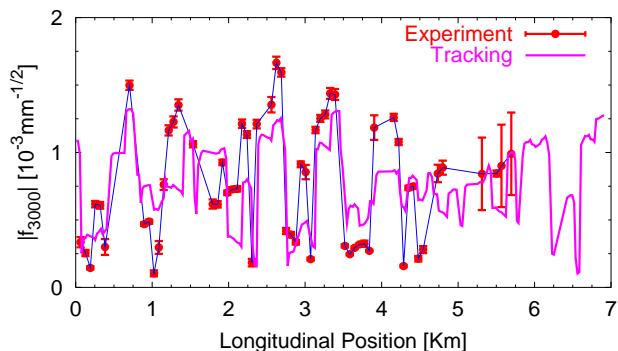


Figure 3: Amplitude of the term f_{3000} versus longitudinal position along the SPS ring from experiment and tracking for the baseline machine.

tracking prediction. The error bars correspond to the errors given by the linear fit. On average, experiment and model agree and the location of the jumps (which correspond to sextupole locations) are the same in both curves. Nevertheless in some regions the curves differ in amplitude.

In another set-up the first four extraction sextupoles were powered to $+30$ A and the following four extraction sextupoles were powered to -30 A. The horizontal tune was moved to 26.69. The beam oscillations were damped due to decoherence, therefore the decoherence factor is applied to compare experiment and model. In fig. 4 (top) the measured amplitude of the sextupolar resonance term f_{3000} is plotted versus the longitudinal position together with a tracking model. The disagreements in this plot requires an improvement of our model. The displacements of the sextupoles with respect to the closed orbit were measured from pick-ups and added to the model. The agreement between the experiment and the new model improved considerably as shown in fig. 4 (bottom). A similar agreement is observed for the other sextupolar resonances. For example the amplitude of the term f_{1200} is shown in fig. 5.

5 CONCLUSIONS

The measurement of linear coupling with the proposed method is now better understood and a new observable has been constructed to obtain more accurate results. For the first time sextupolar resonance terms have been measured at SPS at 26 GeV around the ring. The predicted effects of decoherence on the spectral lines have been confirmed. The beta-beating caused by the closed orbit at the sextupoles has a relevant effect on the resonance terms. The overall agreement between measurement and model is good. Nevertheless some local discrepancies still exist which may indicate the existence of small unknown lattice errors.

6 REFERENCES

[1] A. Schoch, CERN 57–21, (1958).
 [2] M. Berz et al., Part. Accel. **24**, pp. 91–107 (1989).
 [3] A. Bazzani et al., CERN 94–02, (1994).
 [4] O. Brüning et al., Part. Accel. 54, pp. 223–235 (1996).

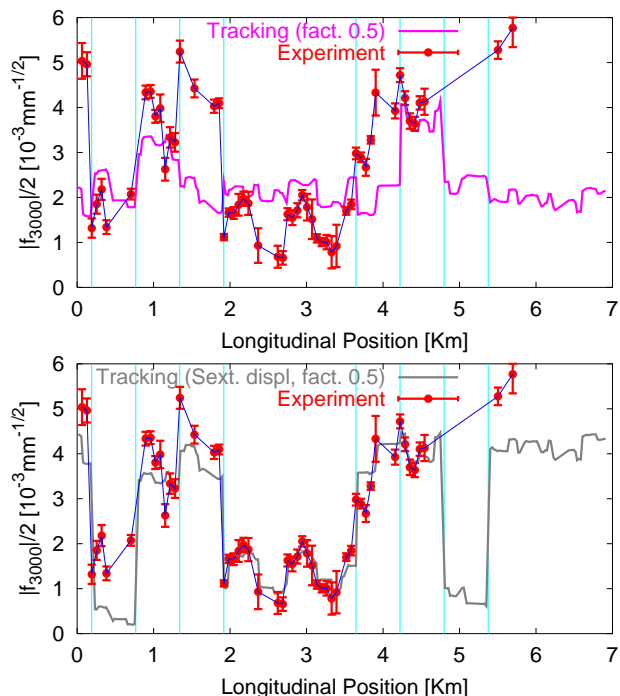


Figure 4: Amplitude of the term f_{3000} versus longitudinal position. Top: Experiment and nominal model with decoherence factor. Bottom: Experiment and model with displaced sextupoles and decoherence factor. The vertical lines show the position of the extraction sextupoles.

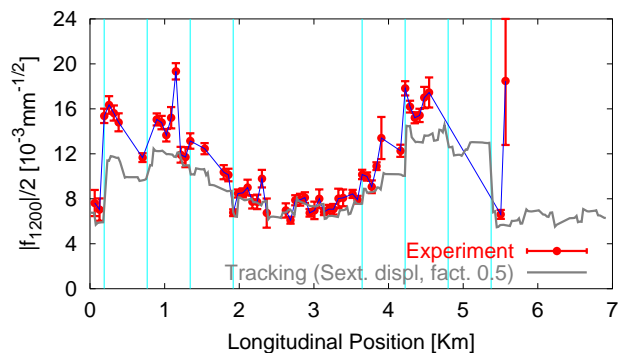


Figure 5: Amplitude of the term f_{1200} versus longitudinal position from experiment and tracking with displaced sextupoles and decoherence factors. The vertical lines show the position of the extraction sextupoles.

[5] J. Bengtsson, CERN 88–05, (1988).
 [6] E. Asseo et al., 4th Euro. Signal Proc. Conf. (1988).
 [7] J. Laskar, Astron. Astrophys. **198**, pp. 341–362 (1988).
 [8] J. Laskar et al., Physica D **56**, pp. 253–269 (1992).
 [9] R. Bartolini and F. Schmidt, AIP Conf. Proc. 395 (1996).
 [10] R. Bartolini and F. Schmidt, Part. Accel. **59**(1998).
 [11] F. Schmidt, R. Tomás, A. Faus-Golfe, PAC 2001 and CERN SL 2001–039.